



# CO<sub>2</sub> adsorption and conversion into cyclic carbonates over a porous ZnBr<sub>2</sub>-grafted N-heterocyclic carbene-based aromatic polymer

Pillaiyar Puthiaraj, Seenu Ravi, Kwangsun Yu, Wha-Seung Ahn\*

Department of Chemistry and Chemical Engineering, Inha University, Incheon, 402-751, South Korea



## ARTICLE INFO

**Keywords:**  
Heterocyclic carbene  
Porous organic polymer  
CO<sub>2</sub> capture  
CO<sub>2</sub> cycloaddition  
Cyclic carbonates

## ABSTRACT

A new nanoporous N-heterocyclic carbene-based cross-linked aromatic polymer (NHC-CAP-1) incorporated with highly nucleophilic bromide anions and with a large surface area was synthesized by a simple Friedel-Crafts reaction of imidazolium salt, triphenylbenzene, and formaldehyde dimethyl acetal. Subsequently, ZnBr<sub>2</sub> was grafted onto the NHC-CAP-1 to obtain NHC-CAP-1(Zn<sup>2+</sup>) with enhanced Lewis acidity. After systematic evaluation of the structural and chemical properties using different analytical techniques, these were explored for CO<sub>2</sub> adsorption and CO<sub>2</sub> chemical fixation to cyclic carbonates. Whilst NHC-CAP-1 showed a high CO<sub>2</sub> capture capacity (188.2 mg g<sup>-1</sup> at 273 K/1 bar) with a moderate CO<sub>2</sub>/N<sub>2</sub> selectivity, NHC-CAP-1(Zn<sup>2+</sup>) displayed significantly enhanced CO<sub>2</sub>/N<sub>2</sub> selectivity (100/80 at 273/298 K) at the expense of diminished CO<sub>2</sub> capture (123.0 mg g<sup>-1</sup> at 273 K/1 bar). These values are among the highest reported so far for porous cross-linked organic polymers. As a catalyst, NHC-CAP-1(Zn<sup>2+</sup>) showed high catalytic activities for CO<sub>2</sub> cycloaddition to a series of epoxides to form cyclic carbonates in the absence of co-catalyst and solvent, producing a high turnover frequency (TOF) of 2202 h<sup>-1</sup> at 100 °C. The effect of reaction parameters including temperature, reaction time, and catalyst loading was examined. NHC-CAP-1(Zn<sup>2+</sup>) could be separated readily and reuse for a minimum of 10 runs while maintaining high activity and stability owing to the strong covalent bonding of Lewis acid Zn<sup>2+</sup> to the NHC-CAP-1 backbones. This work demonstrated that NHC-CAP-1 and NHC-CAP-1(Zn<sup>2+</sup>) are viable porous materials that are highly efficient for both CO<sub>2</sub> capture and catalytic conversion of CO<sub>2</sub> to cyclic carbonates.

## 1. Introduction

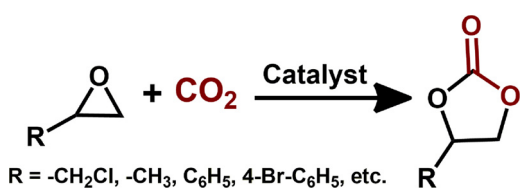
Over the last decade, the global environment has been adversely affected by the rapid rise of CO<sub>2</sub> emissions from fossil-fuel combustion in power plants, automobiles, and other human activities, which led to global warming and ocean acidification [1,2]. At present, CO<sub>2</sub> absorption by liquid amines has been employed in industries for post-synthesis CO<sub>2</sub> capture. However, this approach has the problems of high energy consumption during regeneration, equipment corrosion, low efficiency, and solvent loss [1]. As an alternative, adsorption of CO<sub>2</sub> over amine-functionalized solid support materials has been actively investigated [3,4]. Various porous materials including silica [5], zeolites [6], activated carbons [7], metal organic frameworks [8,9], and porous organic polymers (POPs) [10,11] have been reported for CO<sub>2</sub> capture. Among these, POPs are receiving increased attention because of their large surface area with well-defined pore structure, stable framework, and extended  $\pi$ -conjugation effect [11,12]. To be more specific, many interesting POPs have been reported for CO<sub>2</sub> capture [13–17]. For example, Dai et al. reported triazine-containing task-specific polymers

that adsorbed up to 180.4 mg g<sup>-1</sup> of CO<sub>2</sub> at 273 K/1 bar with CO<sub>2</sub>/N<sub>2</sub> selectivity of 38 [13]. Jiang et al. developed a series of POPs containing N,N,N',N'-tetraphenylbiphenyl-4,4'-diamine- [14] and 1,1,2,2-tetraphenylethane-1,2-diol- [15] moieties, with a maximum CO<sub>2</sub> adsorption of 160 mg g<sup>-1</sup> at 273 K/1 bar and CO<sub>2</sub>/N<sub>2</sub> selectivity of 33. Li et al. reported phenylmethylsilicone-containing POPs with high surface area, showing CO<sub>2</sub> uptake up to 153 mg g<sup>-1</sup> at 273 K/1 bar and CO<sub>2</sub>/N<sub>2</sub> selectivity of 36 [16]. Huang et al. developed an octaphenylcyclotetrasiloxane-containing POP with CO<sub>2</sub> uptake of 64 mg g<sup>-1</sup> at 273 K/1 bar and CO<sub>2</sub>/N<sub>2</sub> selectivity of 11 [17]. It was noticed that the bulk form of these reported POPs has shown only moderate CO<sub>2</sub> capture capacity and CO<sub>2</sub>/N<sub>2</sub> selectivity. Therefore, the design and preparation of new POPs with more CO<sub>2</sub>-philic functional moieties in the structure are desirable to improve the CO<sub>2</sub> capture performances. It is noteworthy that other than the common amine-incorporated materials [3], ionic liquid moieties can also be integrated into a POP structure to enhance the CO<sub>2</sub> adsorption and selectivity, by creating strong electrostatic and van der Waals interactions with CO<sub>2</sub> [18,19].

CO<sub>2</sub> is a non-flammable and useful C1 feedstock for industrial

\* Corresponding author.

E-mail address: [whasahn@inha.ac.kr](mailto:whasahn@inha.ac.kr) (W.-S. Ahn).



**Scheme 1.** Cyclic carbonates synthesis using CO<sub>2</sub> and epoxides.

chemicals [20]. CO<sub>2</sub> fixation into commodity chemicals and fuels under mild reaction conditions is another way to alleviate the global CO<sub>2</sub> problem. In this regard, one of the most interesting CO<sub>2</sub> fixation protocols is the synthesis of cyclic carbonates via an atom-efficient reaction of CO<sub>2</sub> and epoxides (Scheme 1). Cyclic carbonates can be used as a solvent; valuable intermediate for the production of pharmaceuticals, polycarbonates, and polyurethanes; and as electrolytes for Li-secondary batteries [21]. CO<sub>2</sub> cycloaddition to epoxides has been investigated over various kinds of heterogeneous catalysts. In particular, recent reviews of the status of catalytic work [22–26] clearly point out that the CO<sub>2</sub> cycloaddition reaction requires Lewis-acidic/basic sites to bind the epoxide/CO<sub>2</sub>, and high-energy nucleophiles to open the epoxide ring.

POPs are also among the potential catalysts for the cycloaddition of CO<sub>2</sub> to epoxides [27,28], and metal ion-coordinated POPs (e.g., Zn [11,29,30], Co [31], and Al [31]) have been reported to be effective for this purpose. However, all these catalysts needed an external tetrabutylammonium bromide additive to promote the reaction and generally gave unsatisfactory TOFs. To avoid the external additives and to increase the TOFs, Lewis-acidic metal ions-integrated ionic POPs have been tested for CO<sub>2</sub> conversion [19,32]. Ding et al. reported an ionic liquid supported on a Zn-PPh<sub>3</sub>-attached POP catalyst, which yielded 21% conversion of propylene oxide in the cycloaddition of CO<sub>2</sub> (TOF = 1680 h<sup>-1</sup>) at 100 °C. The polymer without Zn also showed 34 mg g<sup>-1</sup> of CO<sub>2</sub> adsorption at 273 K/1 bar [32]. Wang et al. reported an imidazolinium-based porous ionic polymer catalyst with 99% conversion in the presence of ZnBr<sub>2</sub> (equal amount to ionic polymer) as external co-catalyst and N,N'-dimethylformamide (DMF) as solvent at 25 °C after 96 h reaction. The polymer catalyst alone produced cyclic carbonates with TOF of 82.5 h<sup>-1</sup> at 120 °C, and exhibited 128 mg g<sup>-1</sup> of CO<sub>2</sub> adsorption at 273 K/1 bar [19]. These materials, however, required high metal loading, air- and moisture-sensitive phosphine sites, the use of a solvent, and long reaction time to achieve reasonable CO<sub>2</sub> conversion with their low CO<sub>2</sub> adsorption. Therefore, there is a need for a more economical and stable porous ionic polymer with high TOFs and large CO<sub>2</sub> capture capacity for the cycloaddition reaction. To this end, N-heterocyclic carbenes and their metal complexes were recently reported to be promising for various organic transformations. This may lead to the novel synthesis of effective ionic liquid-like POPs, since the NHC-metal bonds are very strong and prevent structural decomposition [33]. Several versatile POPs have been synthesized via different routes by using diverse building blocks [14,28,29,34–37]. Among these reports, Lewis-acid catalyzed Friedel-Crafts reaction of low-cost precursors and formaldehyde dimethyl acetal as a cross-linker has been used recently to prepare a group of POPs that offer many benefits such as easy handling, facile synthesis conditions for scale-up, low-cost, high yield, large surface area, and enhanced stability [14,35]. Bearing these in mind, herein we constructed a new porous N-heterocyclic carbene-based cross-linked aromatic ionic polymer (NHC-CAP-1) from 1,3-di-benzylbenzimidazolium bromide (DBBIBr), triphenylbenzene, and formaldehyde dimethyl acetal through a Friedel-Crafts reaction. Subsequent metalation was carried out using ZnBr<sub>2</sub> (Scheme 2), which further formed strong NHC-Zn bonds in the polymer network. These materials possessed high surface area with suitable micropores to capture a large amount of CO<sub>2</sub> with high selectivity, and mesopores to accelerate the transportation of epoxides and products during catalysis. The NHC-CAP-1(Zn<sup>2+</sup>) catalyst exhibited excellent activity for the conversion of CO<sub>2</sub> to carbonates, with high TOFs and reusability

without the need for any co-catalyst, additive, or solvent.

## 2. Experimental section

### 2.1. Chemicals and reagents

Benzimidazole, benzyl bromide, 1,3,5-triphenylbenzene, formaldehyde dimethyl acetal, anhydrous ferric chloride, KOH, potassium *tert*-butoxide, acetonitrile, dichloromethane, toluene, ethyl acetate, DMF, 1,2-dichloroethane, tetrahydrofuran, ZnBr<sub>2</sub>, ethanol, allyl glycidyl ether, 2-(4-bromophenyl)oxirane, epichlorohydrin, 1,2-epoxy-5-hexene, cyclohexene oxide, propylene oxide, and styrene oxide were obtained from Sigma-Aldrich. All these chemicals were used as received without any additional treatment unless mentioned otherwise. CO<sub>2</sub> (99.999%), CH<sub>4</sub> (99.995%), and N<sub>2</sub> (99.999%) gases were purchased from Daedeok gas Co., Ltd (South Korea).

### 2.2. Preparation of the precursor DBBIBr

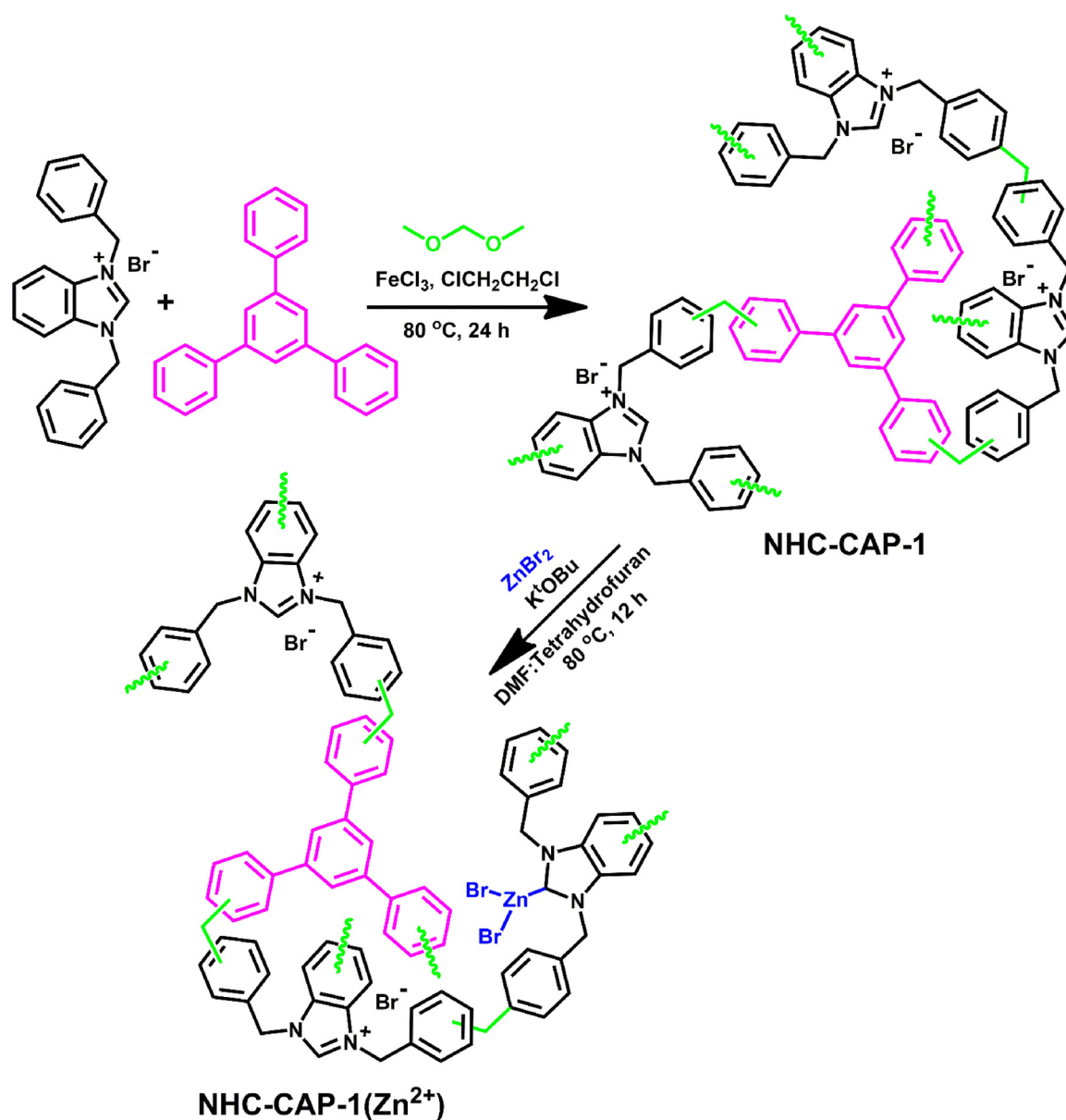
DBBIBr was prepared according to the literature procedure with slight modifications [38]. In a typical synthesis, benzimidazole (15 mmol, 1.77 g) and KOH (16 mmol, 0.9 g) were stirred in acetonitrile (50 mL) at room temperature for 1 h. Benzyl bromide (15 mmol, 1.78 mL) was then added and the reaction mixture was refluxed. After 12 h, the solvent was removed under reduced pressure, and tetrahydrofuran (50 mL) was added and stirred for 15 min to dissolve the organic product. After insoluble KOH and KBr were removed by filtration, the filtrate was concentrated under reduced pressure, and the residual solid was again dissolved in toluene (100 mL). Another portion of benzyl bromide (15 mmol, 1.78 mL) was added into the toluene mixture and stirred at 100 °C for 24 h. The precipitated white powder product was filtered and washed with diethyl ether to yield DBBIBr (87%), which was confirmed by Fourier transform-infrared (FT-IR; Fig. 1) spectroscopy, nuclear magnetic resonance (NMR; Figs. S1–S2) spectroscopy, and elemental analysis (EA; Table 1). FT-IR: 3029 cm<sup>-1</sup> (aromatic C–H), 2930 cm<sup>-1</sup> (–CH<sub>2</sub>–), 1689 cm<sup>-1</sup> (aromatic C=C), 1609 cm<sup>-1</sup> (imidazolium ring C=N), 1550 cm<sup>-1</sup> (imidazolium ring C=C), 1422 cm<sup>-1</sup> (aromatic C–C), 1188 cm<sup>-1</sup> (imidazolium ring C–N<sup>+</sup>); <sup>1</sup>H NMR (400 MHz, DMSO-*d*<sub>6</sub>): *δ* (ppm) = 10.18 (s, 1H, NCHN), 7.99 (dd, 2H, Ar-H), 7.64 (dd, 2H, Ar-H), 7.56–739 (m, 10H, Ar-H), 5.83 (s, 4H, CH<sub>2</sub>); <sup>13</sup>C NMR (100 MHz, DMSO-*d*<sub>6</sub>): *δ* 142.6 (NCN), 133.8, 131.0, 128.8, 128.6, 128.2, 126.6, 113.9 (Ar-C), 49.9 (CH<sub>2</sub>).

### 2.3. Synthesis of NHC-CAP-1

DBBIBr (2 mmol, 0.76 g), 1,3,5-triphenylbenzene (1 mmol, 0.30 g), formaldehyde dimethyl acetal (8 mmol, 0.71 mL) and 1,2-dichloroethane (100 mL) were charged into a 250 mL round-bottom flask and stirred for 15 min at room temperature. Anhydrous ferric chloride (8 mmol, 1.30 g) was then added and the reaction solution was heated to 45 °C with a condenser for 6 h to form the POP network. Then the temperature was raised to 80 °C for 18 h to complete the reaction. After cooling to room temperature, the resultant solid was filtered and washed (2 x 100 mL) with dichloromethane, DMF, ethanol, and water, successively. The solid product was further washed with DMF:ethanol (v/v) for 1 day in a Soxhlet extraction unit, and then dried under reduced pressure for 10 h at 160 °C to obtain NHC-CAP-1 in 94% yield.

### 2.4. Synthesis of NHC-CAP-1(Zn<sup>2+</sup>)

NHC-CAP-1 (1.0 g) was suspended in a DMF:tetrahydrofuran mixture (v/v, 30 mL), and potassium *tert*-butoxide (0.20 g) was added to the solution and stirred at 50 °C for 2 h under nitrogen purged condition. ZnBr<sub>2</sub> (0.070 g) was then added and the solution was heated to 80 °C for 12 h. The solid was filtered and washed with water to remove



**Scheme 2.** Synthesis of NHC-CAP-1 via Friedel-Crafts reaction and the post-synthetic zinc complexation process.

the unreacted base/ $\text{ZnBr}_2$ , and  $\text{KBr}$  (produced from the reaction) dried overnight at  $160^\circ\text{C}$  under reduced pressure to yield 0.98 g of NHC-CAP-1( $\text{Zn}^{2+}$ ).

#### 2.5. General procedure for cyclic carbonates synthesis from $\text{CO}_2$ and epoxides

The conversion of  $\text{CO}_2$  into cyclic carbonates was performed in a stainless-steel high-pressure autoclave furnished with a magnetic bar using the following general procedure. Epoxide (41.5 mmol) and NHC-CAP-1( $\text{Zn}^{2+}$ ) catalyst were charged into the autoclave.  $\text{CO}_2$  gas was then fed at room temperature with a constant pressure of 2 MPa, and the reactor temperature was raised and maintained at  $100^\circ\text{C}$  for 3 h. After cooling to  $10^\circ\text{C}$ , the reactor was depressurized slowly and an internal standard of butyl acetate (5.46 mL) was added by micropipette into the reaction mixture. The resulting mixture was diluted with ethyl acetate (20 mL) and the insoluble catalyst was separated by centrifugation. The supernatant was analyzed using gas chromatography (GC, Agilent Technologies, 7890 A, USA) fitted with an HP-5 capillary column and a flame ionization detector to measure the conversion of

epoxide. Finally, the isolated yield of cyclic carbonates was estimated after purification of the crude product using column chromatography.

#### 2.6. Characterization

The structural information and physicochemical properties of the synthesized materials were inspected by various analytical instruments, and their detailed methods are given in supplementary material.

### 3. Results and discussion

#### 3.1. Characterization of NHC-CAP-1 and NHC-CAP-1( $\text{Zn}^{2+}$ )

An NH-carbene-based aromatic polymer was synthesized directly via a Friedel-Crafts alkylation (electrophilic substitution) reaction between different aromatic monomers (DBBIBr and 1,3,5-triphenylbenzene) and formaldehyde dimethyl acetal as cross-linker. Subsequently,  $\text{ZnBr}_2$  was grafted on NHC-CAP-1 by treating  $\text{ZnBr}_2$  with NHC-CAP-1 in the presence of potassium *tert*-butoxide in a  $\text{DMF}:\text{Tetrahydrofuran}$  mixture, where the  $\text{Zn}^{2+}$  ion was joined to the

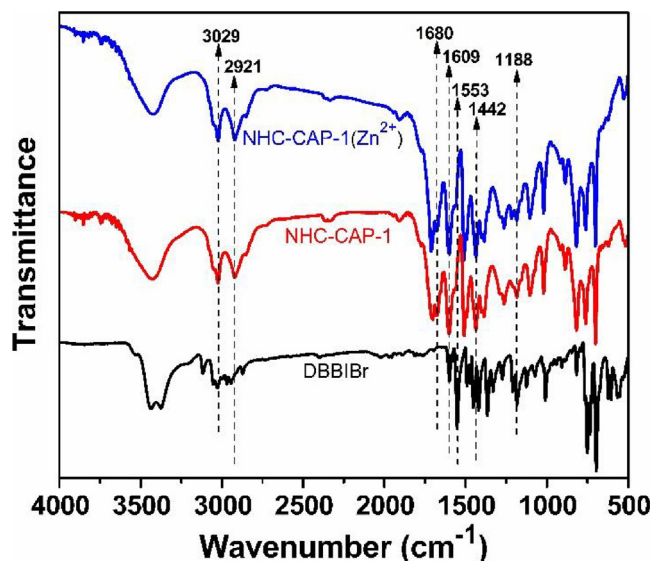


Fig. 1. FT-IR spectra of DBBIBr, NHC-CAP-1, and NHC-CAP-1( $Zn^{2+}$ ).

carbene ( $N=C=N$ ) moiety via a strong covalent bond. The successful growth of the POP network and the correct chemical bonding in it were confirmed using EA, FT-IR solid-state  $^{13}C$  NMR, and X-ray photoelectron spectroscopy (XPS). Table 1 shows the chemical compositions (C, H, and N contents) of DBBIBr, NHC-CAP-1, and NHC-CAP-1( $Zn^{2+}$ ) as quantitatively determined by EA. The high nitrogen content of NHC-CAP-1 suggested that most of DBBIBr was involved in the formation of the network. The nitrogen amount in DBBIBr, NHC-CAP-1, and NHC-CAP-1( $Zn^{2+}$ ) reflecting the imidazole content was 2.63, 1.65, and 1.51 mmol g<sup>-1</sup>, respectively. The bromine content in DBBIBr, NHC-CAP-1, and NHC-CAP-1( $Zn^{2+}$ ) was found to be 2.63, 1.65, and 1.86 mmol g<sup>-1</sup>, respectively, by ion chromatography. The Zn content in NHC-CAP-1( $Zn^{2+}$ ) was found to be 1.61 wt% as inspected by inductively coupled plasma-optical emission spectrometry (ICP-OES). As shown in Fig. 1, the following characteristic FT-IR stretching peaks were found in NHC-CAP-1 and NHC-CAP-1( $Zn^{2+}$ ): (i) an aliphatic C–H vibration peak emanating from  $-\text{CH}_2-$  linkers at 2921 cm<sup>-1</sup>; (ii) bands at 1609, 1553, and 1188 cm<sup>-1</sup> ascribed to imidazolium ring stretching of  $C=N$ ,  $C=C$ , and  $C-N^+$ , respectively; and (iii) bands at 3029, 1680, and 1442 cm<sup>-1</sup> attributed to aromatic phenyl rings stretching of C–H,  $C=C$ , and  $C-C$ , respectively. Solid state  $^{13}C$  CP-MAS NMR spectrum (Fig. S3) of NHC-CAP-1 showed two resonance peaks at around 140 and 128 ppm, corresponding to the substituted and non-substituted (i.e., hydrogen-bearing) aromatic carbons, respectively; and the aliphatic carbon peaks at around 42 and 36 ppm were ascribed to methylene carbon attached to the imidazole moiety and the cross-linker methylene carbon (attached between two phenyl rings) formed from the Friedel-Crafts reaction. The characteristic imidazolium (NCN) carbon peak was overlapped with another peak at ~145 ppm [39]. After metalation, a weak peak of NCN carbon was observed at ~173 ppm, indicating that  $Zn^{2+}$  was grafted on C2 carbon of imidazole moiety in NHC-CAP-

1( $Zn^{2+}$ ) [40].

The chemical structure of DBBIBr, NHC-CAP-1, the grafted Zn species, and their states in NHC-CAP-1( $Zn^{2+}$ ) were further examined by XPS. Fig. S4 shows the C 1 s, N 1 s, and Br 3d XPS data of DBBIBr. Fig. 2 showed the C 1 s, N 1 s, Br 3d, and Zn 2p XPS data of NHC-CAP-1 and NHC-CAP-1( $Zn^{2+}$ ). The C 1 s spectrum of NHC-CAP-1 (Fig. 2(a)) was deconvoluted into five distinct peaks centered at 290.8, 289.0, 286.9, 285.4, and 284.1 eV, which were ascribed to the  $\pi-\pi^*$  transition, imidazolium  $-N-C=N$ , imidazolium C–N, methylene carbon, and aromatic  $C=C$ , respectively [41]. The N 1 s spectrum of NHC-CAP-1 (Fig. 2(b)) showed two different nitrogens of the imidazolium cation (binding energies of 401.8 and 400.7 eV) and trialkylamine (binding energies of 399.6 and 398.6 eV) [42], which shifted slightly from N 1 s XPS of DBBIBr (402.1, 400.9, 400.1, and 398.5 eV). For NHC-CAP-1, the bromide ion binding energy peak (Fig. 2(c)) appeared at 69.7 and 68.5 eV for the Br 3d<sub>3/2</sub> and 3d<sub>5/2</sub> levels, respectively [41], which also shifted from Br 3d<sub>3/2</sub> (70.1 eV) and 3d<sub>5/2</sub> (67.3 eV) of DBBIBr. The deviation of N 1 s and Br 3d binding energy values of NHC-CAP-1 indicated that the network containing nitrogen and bromine are present in the different environment from DBBIBr. After introduction of  $Zn^{2+}$  into the NHC-CAP-1, a new binding energy peak of C 1 s was observed at 283.2 eV (Fig. 2(a)), and the N 1 s imidazolium cation peaks were dramatically reduced (Fig. 2(b)), implying that some of the imidazolium rings was transformed into NH-carbene complex with  $Zn^{2+}$  ion. Concurrently, the binding energy peak at 69.5 eV (Fig. 2(c)) grew dramatically owing to the presence of Zn–Br bonding and bromide ions in NHC-CAP-1( $Zn^{2+}$ ). The Zn 2p spectrum for NHC-CAP-1( $Zn^{2+}$ ) (Fig. 2(d)) revealed the binding energies at 1045.6 and 1022.4 eV for Zn 2p<sub>1/2</sub> and Zn 2p<sub>3/2</sub>, respectively, indicating that the zinc was present in the +2 state [43]. These characterization results indicated the successful synthesis of NHC-CAP-1 and NHC-CAP-1( $Zn^{2+}$ ).

The textural properties of the synthesized networks were examined by  $N_2$  gas adsorption-desorption isotherms at 77 K, and the results are listed in Table 1. Fig. 3(a) depicts a type I isotherm with a sharp  $N_2$  uptake at  $P/P_0 < 0.02$  bar at the beginning followed by an H3 hysteresis loop at high relative pressures ( $0.6 < P/P_0 < 1.0$  bar), indicating that the material has both micro- and mesopores with the interparticle voids [44]. The Brunauer–Emmett–Teller (BET) surface area of NHC-CAP-1 was estimated to be 1433 m<sup>2</sup> g<sup>-1</sup> with a pore volume of 1.40 cm<sup>3</sup> g<sup>-1</sup>. Generally, Friedel-Crafts alkylation is uncontrolled and the reaction takes place both in ortho- and para-position of aromatic moiety. But in the present system, alkylation took place only in the para-position of triphenylbenzene due to the steric nature and the 3D-configuration of triphenylbenzene [45], which produced the uniform polymeric network with large surface area. After grafting  $ZnCl_2$ , the BET surface area and pore volume decreased to 1040 m<sup>2</sup> g<sup>-1</sup> and 1.02 cm<sup>3</sup> g<sup>-1</sup>, respectively, due to partial pore blocking by  $ZnCl_2$  and increased sample mass. These pores of mixed sizes in the networks were confirmed by the obtained pore size distribution curves (Fig. 3(b)). NHC-CAP-1 showed a sharp peak at 1.40 nm, whereas NHC-CAP-1( $Zn^{2+}$ ) showed one at 1.04 nm. Many other peaks with less intensity were also present in the micro- and mesopore region for both materials. The decreased surface area, pore size, and pore volume clearly supported that  $ZnCl_2$  was grafted successfully on the NHC-CAP-

Table 1  
C, N, H, and Zn analyses with the textural properties of the prepared POPs.

Networks	Found (wt%)				Imidazole content <sup>c</sup> (mmol g <sup>-1</sup> )	Br content <sup>d</sup> (mmol g <sup>-1</sup> )	BET surface area (m <sup>2</sup> g <sup>-1</sup> )	Micropore volume <sup>e</sup> (cm <sup>3</sup> g <sup>-1</sup> )	Total pore volume <sup>f</sup> (cm <sup>3</sup> g <sup>-1</sup> )
	C <sup>a</sup>	N <sup>a</sup>	H <sup>a</sup>	Zn <sup>b</sup>					
DBBIBr	66.46	7.37	5.08	–	2.63	2.63	–	–	–
NHC-CAP-1	68.95	4.61	4.93	–	1.65	1.65	1433	0.54	1.40
NHC-CAP-1( $Zn^{2+}$ )	65.81	4.23	4.85	1.61	1.51	1.86	1040	0.40	1.02

<sup>a</sup> Determined from EA; <sup>b</sup>Determined from ICP-OES; <sup>c</sup>Imidazole content was calculated from EA results; <sup>d</sup>Determined from ion chromatography; <sup>e</sup>Micropore volume at  $P/P_0 = 0.1$  bar; <sup>f</sup>Total pore volume at  $P/P_0 = 0.99$  bar.

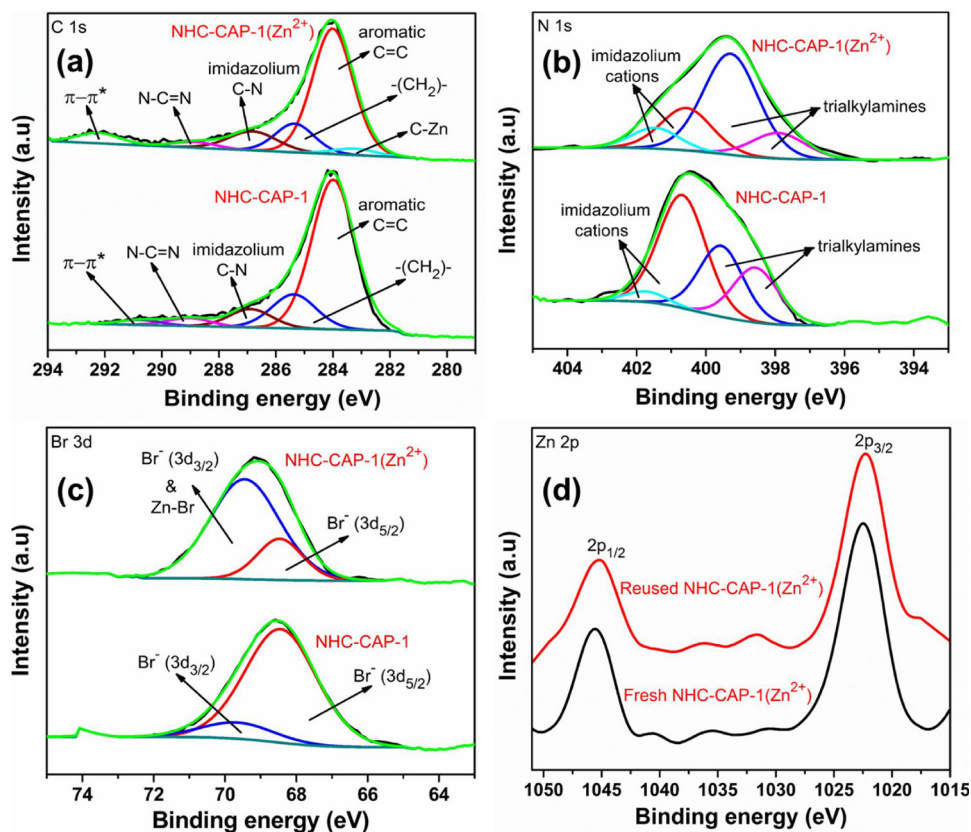


Fig. 2. (a) C 1 s, (b) N 1 s, (c) Br 3d, and (d) Zn 2p XPS binding energies of NHC-CAP-1 and NHC-CAP-1( $Zn^{2+}$ ).

## 1.

Powder X-ray diffraction patterns of the materials (Fig. S5) exhibited broad peaks at 10, 22, and 43°, suggesting their long-range amorphous nature with intrinsic flexibility, disordered linkage, and direct  $\pi$ - $\pi$  interaction between the phenyl moieties [46]. The surface morphology of the porous networks was inspected by electron microscope analysis (Fig. S6). Field emission-scanning electron microscope image (Fig. S6(a–b)) displayed relatively uniform spherical particles in aggregation. Transmission electron microscope (Fig. S6(c–d)) confirmed a porous network made of both micro- and mesopores. Thermogravimetric analysis (Fig. S7) of NHC-CAP-1 and NHC-CAP-1( $Zn^{2+}$ ) showed decomposition at around 270 and 230 °C, respectively.

### 3.2. $CO_2$ , $CH_4$ , and $N_2$ sorption over NHC-CAP-1 and NHC-CAP-1( $Zn^{2+}$ )

The ionic moiety in the structure and the large surface area with

hierarchical pores in NHC-CAP-1 and NHC-CAP-1( $Zn^{2+}$ ) prompted us to examine their gas sorption capacities. Thus their  $CO_2$ ,  $CH_4$ , and  $N_2$  sorption isotherms were analyzed at different temperatures and 1 bar conditions (Fig. 4(a)–(b)). The  $CO_2$  uptakes, the  $CO_2/N_2$ , and  $CO_2/CH_4$  selectivities, and the estimated isosteric heat of adsorption ( $Q_{st}$ ) values are shown in Table 2. Fig. 4(a) shows that the  $CO_2$  uptake of NHC-CAP-1 was 188.2, 133.4, 109.9, and 100.8  $mg\ g^{-1}$  at 273, 288, 298, and 303 K, respectively. As listed in Table S1, these values are higher than those of the most reported POPs. The superior  $CO_2$  sorption is likely due to the high positive charge density and nitrogen atoms in NHC-CAP-1 [19]. After grafting  $ZnCl_2$ , the  $CO_2$  sorption capacities of NHC-CAP-1( $Zn^{2+}$ ) decreased somewhat to 123.0, 91.0, 75.9, and 71.4 at the same conditions (Fig. 4(b)) due to partial pore blocking in NHC-CAP-1 by  $ZnCl_2$ , in accordance with the well-known fact that  $CO_2$  uptake at atmospheric pressure is affected by the surface area, pore size, pore volume, and quadrupole interaction between  $CO_2$  and heteroatom of the

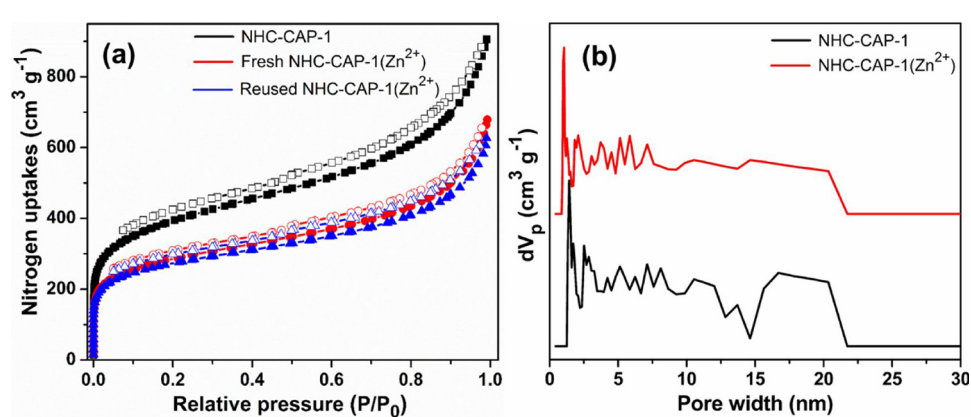


Fig. 3. (a)  $N_2$  isotherms and (b) pore size distributions of NHC-CAP-1 and NHC-CAP-1( $Zn^{2+}$ ).

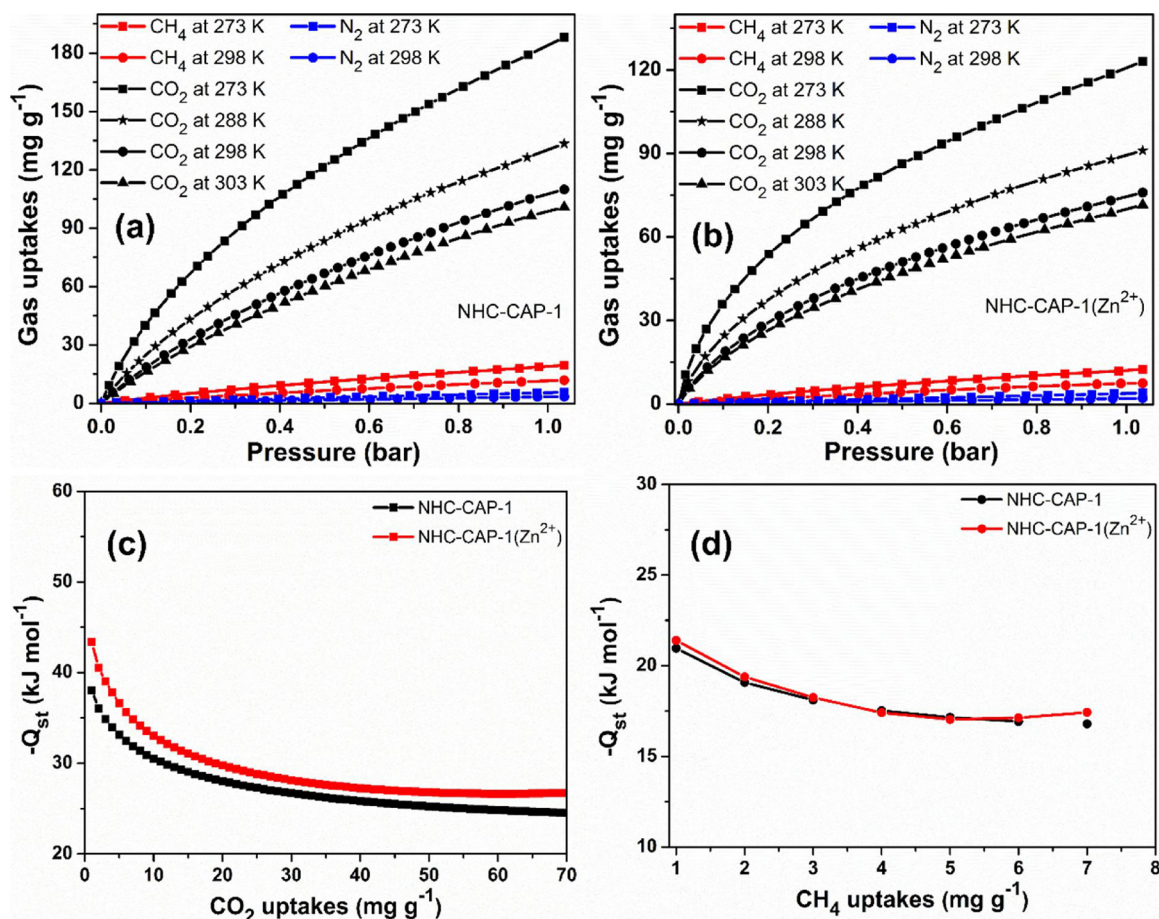


Fig. 4. CO<sub>2</sub>, CH<sub>4</sub>, and N<sub>2</sub> sorption on (a) NHC-CAP-1 and (b) NHC-CAP-1(Zn<sup>2+</sup>), and the isosteric heat of adsorption for (c) CO<sub>2</sub> and (d) CH<sub>4</sub> for NHC-CAP-1 and NHC-CAP-1(Zn<sup>2+</sup>).

pore walls [3,47]. The N<sub>2</sub> sorption capacities of NHC-CAP-1 and NHC-CAP-1(Zn<sup>2+</sup>) were also measured at 273 and 298 K (Fig. 4(a)–(b)) to estimate the CO<sub>2</sub>/N<sub>2</sub> selectivity. Under 1 bar, the N<sub>2</sub> sorption capacities were 5.7/3.4 and 3.9/2.1 mg g<sup>-1</sup> at 273/298 K for NHC-CAP-1 and NHC-CAP-1(Zn<sup>2+</sup>), respectively. The CO<sub>2</sub> selectivity over CH<sub>4</sub> or N<sub>2</sub> were evaluated using Henry's initial slope method from single-component gas sorption isotherms at 273 and 298 K in the pressure region of the 0–0.2 bar, and the values are summarized in Table 2. The estimated selectivity of NHC-CAP-1 for CO<sub>2</sub> over N<sub>2</sub> was 69 and 52 at 273 and 298 K, respectively (Fig. S8(a)–(b)). After grafting of ZnBr<sub>2</sub> on NHC-CAP-1, the corresponding CO<sub>2</sub>/N<sub>2</sub> selectivity was enhanced to 100 and 80 (Fig. S8(c)–(d)). The high CO<sub>2</sub> selectivity over N<sub>2</sub> in NHC-CAP-1(Zn<sup>2+</sup>) is likely due to the formation of carbamate salt via strong acid-base chemisorption between CO<sub>2</sub> and the basic tertiary nitrogen atoms as confirmed by FT-IR (Fig. S9) [48] and the possible formation of CO<sub>2</sub> coordinated zinc complex [49]. These selectivity values are higher than those of recently reported POPs listed in Table S1. We also determined the CH<sub>4</sub> sorption capacities of NHC-CAP-1 and NHC-CAP-1(Zn<sup>2+</sup>) at

273/298 K and 1 bar (Fig. 4(a)–(b)) to be 19.5/11.8 and 12.5/7.5 mg g<sup>-1</sup>, respectively. Fig. S8 (a)–(d) shows the corresponding CO<sub>2</sub>/CH<sub>4</sub> selectivities of 15/13 and 22/20 at 273/298 K. These results suggest that the carbene-based networks are potential adsorbents for CO<sub>2</sub> capture with high capacity and good selectivity over N<sub>2</sub> and CH<sub>4</sub>.

The heat of adsorption (Q<sub>st</sub>) of CO<sub>2</sub> and CH<sub>4</sub> on the two adsorbents was measured by the Clausius-Clapeyron Eq. (1), using the measured CO<sub>2</sub> and/or CH<sub>4</sub> sorption isotherms at three different temperatures between 273 and 298 K.

$$Q_{st} = -R \left[ \frac{\partial \ln P}{\partial \left( \frac{1}{T} \right)} \right]_{\theta} \quad (1)$$

where  $\theta$  = fraction of the adsorbed sites at a pressure P and temperature T; and R = universal gas constant. Fig. 4(c) exhibits that the -Q<sub>st</sub> values of CO<sub>2</sub> for NHC-CAP-1 and NHC-CAP-1(Zn<sup>2+</sup>) were 38.0 and 43.3 kJ mol<sup>-1</sup> at 1 mg g<sup>-1</sup>, respectively, and decreased to 24.5 and 26.7 kJ mol<sup>-1</sup> as the adsorbed CO<sub>2</sub> reached at 70 mg g<sup>-1</sup>. The initial

Table 2

CO<sub>2</sub>, N<sub>2</sub>, and CH<sub>4</sub> uptakes, selectivities (CO<sub>2</sub>/N<sub>2</sub> and CO<sub>2</sub>/CH<sub>4</sub>), and binding affinity of CO<sub>2</sub> and CH<sub>4</sub> for the synthesized materials.

Networks	CO <sub>2</sub> uptakes (mg g <sup>-1</sup> )				CH <sub>4</sub> uptake (mg g <sup>-1</sup> )		N <sub>2</sub> uptakes (mg g <sup>-1</sup> )		CO <sub>2</sub> /N <sub>2</sub> selectivity <sup>a</sup>		CO <sub>2</sub> /CH <sub>4</sub> selectivity <sup>a</sup>		-Q <sub>st</sub> for CO <sub>2</sub>	-Q <sub>st</sub> for CH <sub>4</sub>		
	273K		288K		298K		303K		273K		298K					
	1 bar	1 bar	1 bar	1 bar	1 bar	1 bar	1 bar	1 bar	273K	298K	273K	298K				
NHC-CAP-1	188.2	133.4	109.9	100.8	19.5	11.8	5.7	3.4	69:1	52:1	15:1	13:1	38.0-24.5	20.9-16.7		
NHC-CAP-1(Zn <sup>2+</sup> )	123.0	91.0	75.9	71.4	12.5	7.5	3.9	2.1	100:1	80:1	22:1	20:1	43.3-26.7	21.3-17.4		

<sup>a</sup> Adsorption selectivity based on Henry's law.

**Table 3**  
Cycloaddition of  $\text{CO}_2$  to epichlorohydrin over NHC-CAP-1( $\text{Zn}^{2+}$ ).<sup>a</sup>

Entry	Catalyst (mg)	Temp (°C)	Conversion (%) <sup>b</sup>	TOFs
1	–	60	< 3	–
2	NHC-CAP-1	60	< 7	–
3	NHC-CAP-1( $\text{Zn}^{2+}$ )	60	15	275
4	NHC-CAP-1( $\text{Zn}^{2+}$ )	80	35	786
5	NHC-CAP-1( $\text{Zn}^{2+}$ )	90	64	1439
6	NHC-CAP-1( $\text{Zn}^{2+}$ )	100	97	2181
7	NHC-CAP-1	100	59	–
8 <sup>c</sup>	DBBIBr	100	36	–
9 <sup>c,d</sup>	DBBIBr/ $\text{ZnBr}_2$	100	82	1844
10 <sup>d</sup>	NHC-CAP-1/ $\text{ZnBr}_2$	100	90	2024

<sup>a</sup> Reaction conditions: Epichlorohydrin (41.5 mmol), 2 MPa  $\text{CO}_2$  pressure, catalyst (25 mg where 1.61 wt% of Zn), 3 h; <sup>b</sup>conversion was determined by GC using butyl acetate as the internal standard; <sup>c</sup>25 mg of DBBIBr; <sup>d</sup>1.4 mg (1.61 wt % of Zn) of  $\text{ZnBr}_2$ .

$Q_{\text{st}}$  values are comparable with the reported values for some porous materials: PPN-6-CH<sub>2</sub>-TETA (63 kJ mol<sup>-1</sup>) [4], MTF-Mg (46 kJ mol<sup>-1</sup>) [50], 3-aminopropyl-immobilized SBA-15 (72 kJ mol<sup>-1</sup>) [51], and ethylenediamine-immobilized  $\text{H}_3[\text{Cu}_4\text{Cl}_3\text{-}(\text{BTTRi})_8]$  MOF (63 kJ mol<sup>-1</sup>) [52]. The higher value of  $Q_{\text{st}}$  for  $\text{CO}_2$  on NHC-CAP-1( $\text{Zn}^{2+}$ ) must be due to the presence of basic tertiary nitrogen atoms (2,3-dihydrobenzimidazole moiety) and the narrower pore size (~1.04 nm) than the NHC-CAP-1 (~1.40 nm). The  $Q_{\text{st}}$  values for  $\text{CH}_4$  (Fig. 4(d)) were calculated to be 20.9–16.7 and 21.3–17.4 kJ mol<sup>-1</sup> at the loading levels of 1–7 mg g<sup>-1</sup> for NHC-CAP-1 and NHC-CAP-1( $\text{Zn}^{2+}$ ), respectively.

### 3.3. $\text{CO}_2$ conversion into cyclic carbonates

The large surface area, mesoporosity, bromide-rich skeleton, and

high  $\text{CO}_2$  sorption capacities of NHC-CAP-1 and NHC-CAP-1( $\text{Zn}^{2+}$ ) indicated their high potential as a catalyst for liquid phase  $\text{CO}_2$  fixation reactions, such as the cycloaddition of  $\text{CO}_2$  with epoxides. Thus, epichlorohydrin was chosen as a model epoxide, and the experimental results are shown in Table 3. Firstly, the reaction was carried out under relatively mild conditions (60 °C and 2 MPa  $\text{CO}_2$  pressure) to monitor the general trend. While negligible epoxide conversion (ca. 3%) was detected under catalyst-free condition (Table 3, entry 1), a slightly higher conversion of 7% was obtained for the NHC-CAP-1 catalyst (Table 3, entry 2). The conversion further increased to 15% for NHC-CAP-1( $\text{Zn}^{2+}$ ) (Table 3, entry 3), indicating the contribution of the Lewis-acidity towards the cycloaddition reaction. As the reaction temperature increased, 35% conversion with  $\text{TOF} = 786 \text{ h}^{-1}$  at 80 °C (Table 3, entry 4), 64% conversion with  $\text{TOF} = 1439 \text{ h}^{-1}$  at 90 °C (Table 3, entry 5), and 97% conversion with  $\text{TOF} = 2181 \text{ h}^{-1}$  at 100 °C (Table 3, entry 6) were obtained. The ionic NHC-CAP-1 polymer showed 59% conversion at 100 °C (Table 3, entry 7) probably aided by the presence of C2-H of imidazolium salt with acidic nature [53], bromide anion, and nanoporous structure, whereas the reaction with the monomer unit of DBBIBr showed 36% conversion of epoxide (Table 3, entry 8), and the physical mixture of DBBIBr/ $\text{ZnBr}_2$  exhibited 82% conversion of epoxide with  $\text{TOF} = 1844 \text{ h}^{-1}$  (Table 3, entry 9) due to the formation of [DBBIBr] $[\text{ZnBr}_3]$  complex [54]. The enhancement of the catalytic activity of NHC-CAP-1( $\text{Zn}^{2+}$ ) for the cycloaddition reaction is owing to the combined contribution from several factors: the presence of high complexing ability of Lewis acidic  $\text{Zn}^{2+}$  ion; C2-H of imidazolium salt with acidic nature; the high nucleophilicity/leaving ability of bromide anions (due to the weak imidazolium cation–bromide anion interaction as shown by XPS); basic nitrogen atom; and the confined nanoporous environment. The large surface area with micro-porosity and the basic tertiary nitrogen atom in NHC-CAP-1( $\text{Zn}^{2+}$ ) can enhance the  $\text{CO}_2$  sorption and the  $\text{CO}_2$  bound nitrogen atom is also

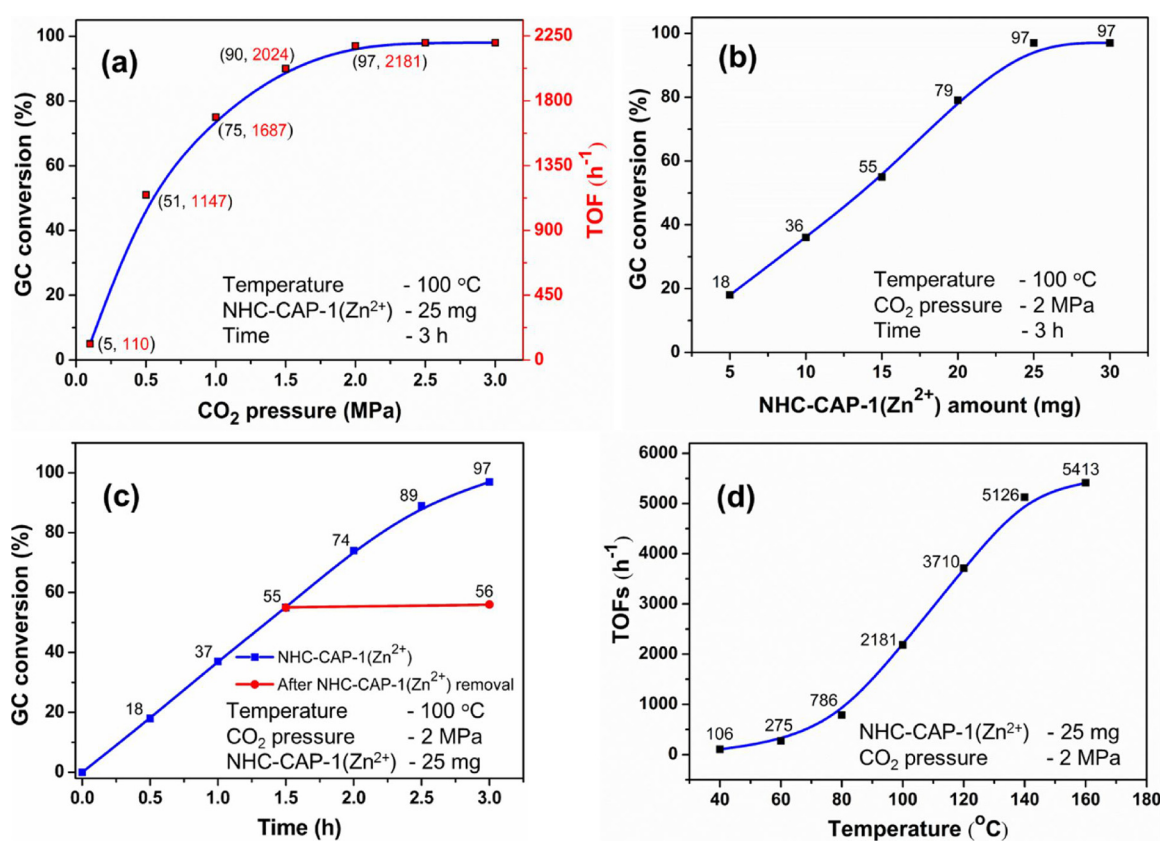


**Fig. 5.** Effect of reaction parameters on the  $\text{CO}_2$  cycloaddition reaction over NHC-CAP-1( $\text{Zn}^{2+}$ ): (a)  $\text{CO}_2$  pressure on TOFs, (b) catalyst loading, (c) reaction time, and (d) temperature on TOFs after 1 h reaction.

located next to the  $Zn^{2+}$  ion, and the mesoporosity increases the diffusion of epoxide to the catalytically active  $Zn^{2+}$  ions (see mechanism later). The physical mixture of NHC-CAP-1 and  $ZnBr_2$  was also tested, which showed 90% conversion (Table 3, entry 10) due to the availability of acidic C2-H of imidazolium salt [53] and a formation of a small portion of tribromozincate complex in NHC-CAP-1 ([NHC-CAP-1]  
[ $ZnBr_3$ ]) [54]. When  $ZnBr_2$  was grafted to the NHC-CAP-1 polymer (NHC-CAP-1( $Zn^{2+}$ )), the heterogeneous reaction mixture made the product separation simple, and it was not necessary to replace the  $ZnBr_2$  in the recycle runs (to be shown later).

The influence of  $CO_2$  pressure, NHC-CAP-1( $Zn^{2+}$ ) loading, reaction time, and temperature on the reaction was then examined more closely, and the results are shown in Figs. 5 & S10. When the  $CO_2$  pressure was increased from 0.1 to 2 MPa (Figs. 5(a) & S10(a)), the yield of 4-chloromethyl-[1,3]dioxolan-2-one as product increased from 5% to 97%, due to the increased sorption of  $CO_2$  on the basic tertiary nitrogen atoms (2,3-dihydrobenzimidazole moiety) in the high surface area NHC-CAP-1( $Zn^{2+}$ ). Further increasing the pressure to 3 MPa produced little increase in product yield. As shown in Figs. 5(b) & S10(b), increasing the catalyst loading from 5 to 10, 15, 20, and 25 mg increased the conversion of epichlorohydrin from 18 to 36, 55, 79, and 97, respectively, while a further increase of the catalyst had little effect on conversion. The kinetic profile of the reaction in Fig. 5(c) shows that the conversion of epichlorohydrin increased almost linearly with time up to 3 h. The conversions of epichlorohydrin at different time intervals were also monitored by NMR spectroscopy in Fig. S11, which showed good agreement with the GC results, namely 56% and > 98% conversion at 1.5 and 3 h, respectively. In addition, we did not observe any extra peaks of hydroxy-derivative side products (1-bromo-3-chloropropan-2-ol and 2-bromo-3-chloropropan-1-ol) in the reaction mixture at 1.5 h (Fig. S11), which implied that the bromide nucleophile attack primarily took place on the less-hindered carbon of the epoxide due to the bulky nature of bromide ion at high reaction temperature. As shown in Figs. 5(d) & S10(c), NHC-CAP-1( $Zn^{2+}$ ) became more active at above 60 °C, and the TOF increased rapidly and reached 5413 h<sup>-1</sup> at 160 °C, which imply that the activation of the nucleophilic bromide anion in NHC-CAP-1( $Zn^{2+}$ ) is difficult at below 60 °C.

The reaction kinetics at different  $CO_2$  pressures (Fig. S10(a)) and at different loadings of NHC-CAP-1( $Zn^{2+}$ ) catalyst (Fig. S10(b)), respectively, were then investigated under solvent-free reaction condition with epichlorohydrin as a substrate to measure the reaction rates. The rate equation is given by Eq. (2) [55]. The process followed the first order kinetics with respect to epoxide (Fig. S12). We then studied the dependence on  $CO_2$  pressure (Fig. S13(a)) and on NHC-CAP-1( $Zn^{2+}$ ) loading (Fig. S13(b)) under the fixed epichlorohydrin concentration (41.5 mmol) and temperature (100 °C). The simplified reaction rate is given in Eq. (3).

$$rate = k [epoxide]^a [CO_2]^b [catalyst]^c \quad (2)$$

$$rate = k_{obs} [epoxide]^a, \text{ where } k_{obs} = k [CO_2]^b [catalyst]^c \quad (3)$$

$$\ln (k_{obs}) = \ln (A) - \left( \frac{E_{a-app}}{R} \right) \left( \frac{1}{T} \right) \quad (4)$$

where  $k$  is the rate constant and  $E_{a-app}$  is the apparent activation energy.

The order of the reaction with respect to  $CO_2$  and NHC-CAP-1( $Zn^{2+}$ ) was found to be 0.92 and 1.89, respectively (Fig. S13(c-d)), implying that one molecule of  $CO_2$  and two different sites ( $Zn^{2+}$  and  $Br^-$ ) in NHC-CAP-1( $Zn^{2+}$ ) are involved in the  $CO_2$  cycloaddition reaction as we proposed in the reaction mechanism (see later). The activation energy ( $E_a$ ) of the reaction was estimated by Arrhenius Eq. (4) [56] using the obtained reaction kinetics at different temperatures between 60 and 160 °C (Figs. S10(c) & S14(a)). Two regions were shown in the Arrhenius plot (Fig. S14(b)). The  $E_a$  was found to be 12.62 and 4.10 kcal mol<sup>-1</sup> at 60–100 °C and 120–160 °C, respectively, which agreed closely with the theoretical calculation of  $E_a$  in the  $CO_2$

cycloaddition reaction with propylene oxide in the presence of  $Zn-PPh_3$ -attached POP catalyst [32]. The obtained  $E_a$  values seem to imply that catalytically reactive species (imidazolium and bromide ions) in NHC-CAP-1( $Zn^{2+}$ ) are increasingly separated at high reaction temperatures to promote the reaction better because the bromide nucleophile can attack the less hindered epoxide carbons more easily when imidazolium and bromide ions are separated.

A leaching test was carried out in the optimized reaction conditions (Fig. 5(c)) to confirm the heterogeneous nature of NHC-CAP-1( $Zn^{2+}$ ). The reaction was stopped at 1.5 h, the reactor was cooled to 10 °C, and the reactor was depressurized slowly. The catalyst was separated using WHATMAN filter (0.45 µm pore), the collected supernatant liquid was transferred to a new reactor, and the reaction was continued under the same reaction condition for an additional 1.5 h. Notably, the final filtrate solution did not show any further conversion of epichlorohydrin and no  $Zn^{2+}$  leaching was detected in the filtrate solution by ICP analysis, which proves the heterogeneity of NHC-CAP-1( $Zn^{2+}$ ) catalyst in the present system and also confirmed that the  $Zn^{2+}$  was grafted strongly on the NHC-CAP-1.

The stability of [NHC-CAP-1]  
[ $ZnBr_3$ ] (physically mixed NHC-CAP-1 and  $ZnBr_2$ ) and NHC-CAP-1( $Zn^{2+}$ ) catalysts was also tested in recycling runs under the following optimized conditions: epichlorohydrin (41.5 mmol), catalyst (25 mg), 2 MPa  $CO_2$  pressure, 100 °C, and 3 h. After completing the reaction in each cycle, the catalyst was separated by centrifugation, washed with water, dried, and reused for repeated runs. The epichlorohydrin was adjusted with respect to the amount of NHC-CAP-1( $Zn^{2+}$ ) / [NHC-CAP-1]  
[ $ZnBr_3$ ] recovered after each reaction cycle. As shown in Fig. 6, NHC-CAP-1( $Zn^{2+}$ ) could be reused without noticeable loss of activity for 10 consecutive runs. Whereas [NHC-CAP-1]  
[ $ZnBr_3$ ] activity was dropped steadily in the consecutive runs due to the leaching of  $Zn^{2+}$  ion from the catalyst. These results clearly proved that the covalently grafted  $Zn^{2+}$  on NHC-CAP-1 (NHC-CAP-1( $Zn^{2+}$ )) was highly stable compared to that of the physical mixture complex of [NHC-CAP-1]  
[ $ZnBr_3$ ]. The used NHC-CAP-1( $Zn^{2+}$ ) was further characterized using XPS,  $N_2$  sorption isotherm, and ICP-OES techniques. The XPS data and  $N_2$  sorption isotherm of used NHC-CAP-1( $Zn^{2+}$ ) after 10 cycles remained close to those of the fresh catalyst (Figs. 2(d) and 3 (a)). The Zn content in the used NHC-CAP-1( $Zn^{2+}$ ) catalyst was found to be 1.58 wt% based on ICP-OES, which was almost same as for the fresh one, confirming that Zn was strongly incorporated in the NHC-CAP-1 polymer framework.

The effectiveness of NHC-CAP-1( $Zn^{2+}$ ) for the cycloaddition of different epoxide substrates under the optimized conditions was studied, and the results are presented in Fig. 7. The obtained cyclic carbonates were confirmed by  $^1H$  and  $^{13}C$  NMR in Fig. S15–S28. The

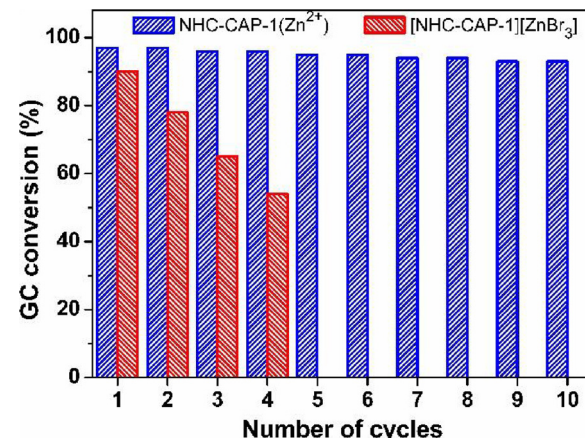
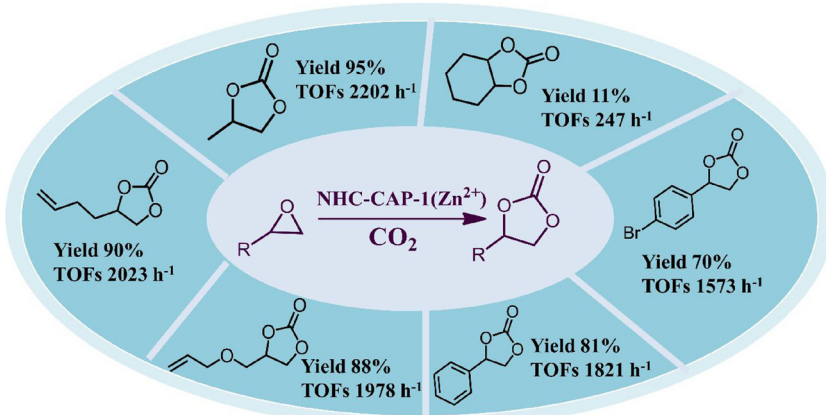
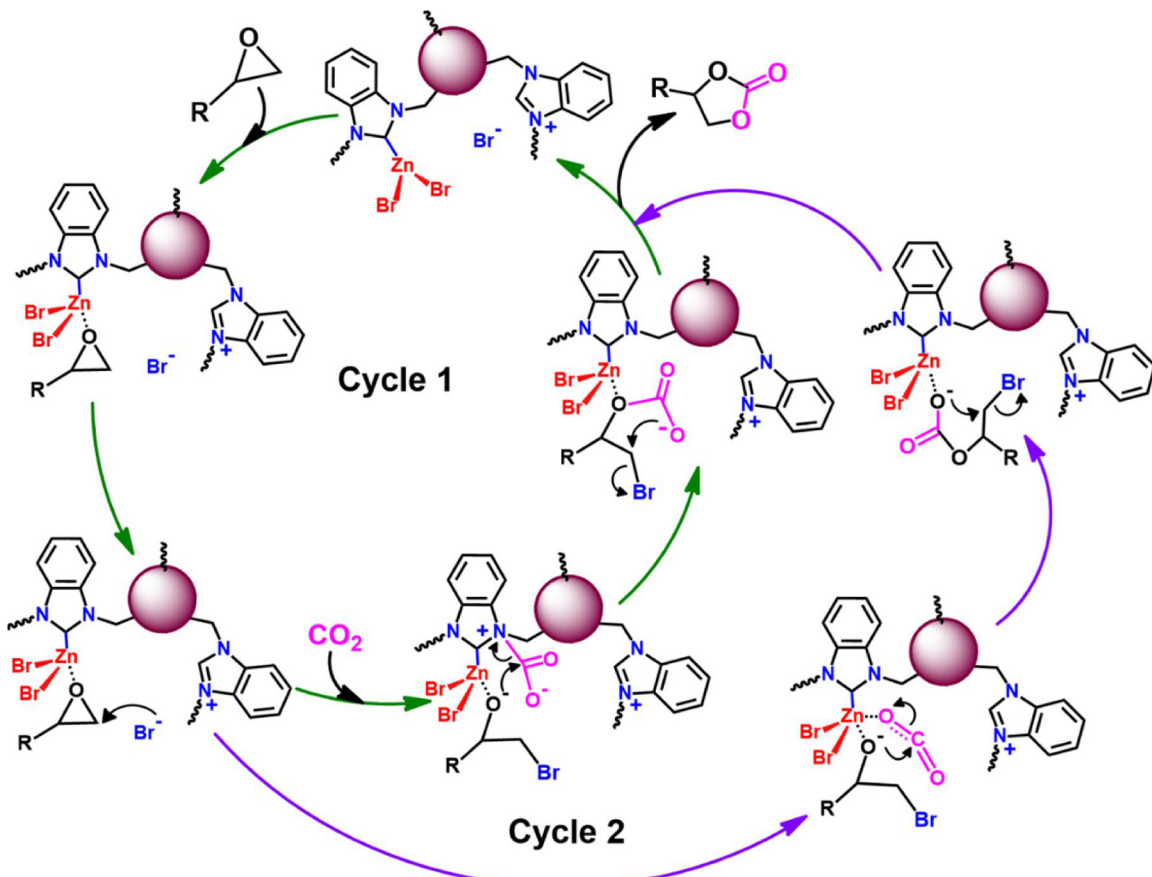


Fig. 6. Recycling test of NHC-CAP-1( $Zn^{2+}$ ) and [NHC-CAP-1]  
[ $ZnBr_3$ ] for the cycloaddition of  $CO_2$  with epichlorohydrin under the optimized reaction conditions.

Fig. 7. Cycloaddition of  $\text{CO}_2$  with different epoxides over NHC-CAP-1( $\text{Zn}^{2+}$ ).Fig. 8. Proposed reaction mechanism for the cycloaddition of  $\text{CO}_2$  and epoxides over NHC-CAP-1( $\text{Zn}^{2+}$ ).

reaction of all the aliphatic terminal epoxides with  $\text{CO}_2$  gave the corresponding cyclic carbonates in excellent yields with high TOFs. Similarly, the aromatic terminal epoxides of styrene oxide and 2-(4-bromophenyl)oxirane having larger molecular sizes also produced respective cyclic carbonates with TOF of 1821 and  $1573 \text{ h}^{-1}$ , respectively, which highlighted the importance of mesoporosity in the catalyst network for the cycloaddition reaction. Only the internal epoxide, cyclohexene oxide, exhibited a low yield due to the high steric hindrance at the ring-opening carbon [57].

The efficiency of NHC-CAP-1( $\text{Zn}^{2+}$ ) catalyst in terms of TOF was compared with recently reported benchmark POPs (Table S2). NHC-CAP-1( $\text{Zn}^{2+}$ ) clearly has a higher TOF than the other catalysts without co-catalyst or solvent and at a lower reaction temperature. The high

$\text{CO}_2$  sorption capacity of NHC-CAP-1( $\text{Zn}^{2+}$ ) in its hierarchical pore structure, the presence of nucleophilic  $\text{Br}^-$  ions, and the incorporation of the Lewis acid  $\text{Zn}^{2+}$  on the carbene unit of the polymer all contributed to the excellent catalytic performance in a solvent- and co-catalyst-free environment.

Based on our experimental results and the previous literature [19,32,49,58], a plausible reaction mechanism could be proposed for the catalytic conversion of epoxide and  $\text{CO}_2$  to cyclic carbonates over NHC-CAP-1( $\text{Zn}^{2+}$ ) (Fig. 8). The attack of a nucleophile (halide anion) on epoxide is known as the rate-determining step in the cycloaddition of  $\text{CO}_2$  with epoxide [19,58]. The Br XPS result of NHC-CAP-1( $\text{Zn}^{2+}$ ) showed doublet peaks at  $\sim 69.5$  ( $3\text{d}_{3/2}$ ) and  $68.5$  eV ( $3\text{d}_{5/2}$ ) related to the  $\text{Br}^-$  species (Fig. 2(c)). These peaks were strongly down-shifted

from the neutral bromide (71–72 eV) [19], suggesting the weak imidazolium cation – bromide anion interaction in the NHC-CAP-1( $Zn^{2+}$ ) catalyst. The bromide anion with good leaving ability can easily attack the less hindered carbon of the epoxide. Under these circumstances, the epoxide is first activated by the Lewis acidic  $Zn^{2+}$  center in NHC-CAP-1( $Zn^{2+}$ ), and the nucleophilic  $Br^-$  anion attacks the less hindered carbon of the epoxide to produce an oxyanion intermediate. In the first case (cycle 1), nitrogen sites in NHC-CAP-1( $Zn^{2+}$ ) adsorb  $CO_2$  to form a zwitterionic carbamate salt (See FT-IR in Fig. S9) and nucleophilic addition of the oxyanion intermediate to the carbon of the carbamate salt takes place. Simultaneously, intramolecular ring-closing of the carbonate anion intermediate takes place to form the cyclic carbonate and regeneration of NHC-CAP-1( $Zn^{2+}$ ). In the second case (cycle 2), the Lewis acidic  $Zn^{2+}$  centers of NHC-CAP-1( $Zn^{2+}$ ) adsorb  $CO_2$  leading to the formation of  $CO_2$  coordinated zinc complex [49], which permits the intermolecular nucleophilic addition of the oxyanion intermediate to form a metal carbonate intermediate. Subsequently, intramolecular ring-closing of the carbonate anion intermediate yields the cyclic carbonates as before, which regenerates the NHC-CAP-1( $Zn^{2+}$ ) for the next run.

#### 4. Conclusions

An N-heterocyclic carbene-based cross-linked aromatic polymer incorporated with nucleophilic bromide anions and with a large surface area (NHC-CAP-1) was prepared by a simple Friedel-Crafts reaction, and post-synthetically grafted with  $ZnBr_2$  to produce NHC-CAP-1( $Zn^{2+}$ ). NHC-CAP-1 showed excellent  $CO_2$  capture of 188.2 mg g<sup>-1</sup> under 1 bar and moderate  $CO_2/N_2$  selectivity of 69 at 273 K, and the  $CO_2/N_2$  selectivity at 273 K was further enhanced to 100 in NHC-CAP-1( $Zn^{2+}$ ). NHC-CAP-1( $Zn^{2+}$ ) showed superior catalytic performance with high yields and TOF in the  $CO_2$  cycloaddition reaction with various epoxides, affording the corresponding cyclic carbonates at 100 °C and 2 MPa  $CO_2$  pressure without using any co-catalyst or solvent. Further, the catalyst could be recovered easily and reused for at least 10 times without diminishing its outstanding activity, owing to the presence of high bromide nucleophile, the strong covalent bond between NHC-carbene carbon and Lewis acidic  $Zn^{2+}$  ions, and the coexistence of micro- and mesoporosity.

#### Acknowledgements

This work was supported by the Basic Science Research Program through the National Research Foundation of Korea (NRF) funded by the Ministry of Education (2015R1A4A1042434) and also by C1 Gas Refinery Program (2015M3D3A1A01064899) by the Ministry of Science, ICT & Future Planning.

#### Appendix A. Supplementary data

Supplementary material related to this article can be found, in the online version, at doi:<https://doi.org/10.1016/j.apcatb.2019.03.076>.

#### References

- [1] R.S. Haszeldine, Carbon capture and storage: how green can black be? *Science* 325 (2009) 1647–1652.
- [2] Y. Fu, X. Zhu, L. Huang, X. Zhang, F. Zhang, W. Zhu, Azine-based covalent organic frameworks as metal-free visible light photocatalysts for  $CO_2$  reduction with  $H_2O$ , *Appl. Catal. B: Environ.* 239 (2018) 46–51.
- [3] P. Puthiaraj, Y.-R. Lee, W.-S. Ahn, Microporous amine-functionalized aromatic polymers and their carbonized products for  $CO_2$  adsorption, *Chem. Eng. J.* 319 (2017) 65–74.
- [4] W. Lu, J.P. Sculley, D. Yuan, R. Krishna, Z. Wei, H.-C. Zhou, Polyamine-tethered porous polymer networks for carbon dioxide capture from flue gas, *Angew. Chem., Int. Ed.* 51 (2012) 7480–7484.
- [5] Y. Belmabkhout, R. Serna-Guerrero, A. Sayari, Adsorption of  $CO_2$  from dry gases on MCM-41 silica at ambient temperature and high pressure. 1: pure  $CO_2$  adsorption, *Chem. Eng. Sci.* 64 (2009) 3721–3728.
- [6] T.-H. Bae, M.R. Hudson, J.A. Mason, W.L. Queen, J.J. Dutton, K. Sumida, K.J. Micklash, S.S. Kaye, C.M. Brown, J.R. Long, Evaluation of cation-exchanged zeolite adsorbents for post-combustion carbon dioxide capture, *Energy Environ. Sci.* 6 (2013) 128–138.
- [7] Y. Li, B. Zou, C. Hu, M. Cao, Nitrogen-doped porous carbon nanofiber webs for efficient  $CO_2$  capture and conversion, *Carbon* 99 (2016) 79–89.
- [8] Z. Zhang, Z.-Z. Yao, S. Xiang, B. Chen, Perspective of microporous metal–organic frameworks for  $CO_2$  capture and separation, *Energy Environ. Sci.* 7 (2014) 2868–2899.
- [9] Z.-R. Jiang, H. Wang, Y. Hu, J. Lu, H.-L. Jiang, Polar group and defect engineering in a metal–organic framework: synergistic promotion of carbon dioxide sorption and conversion, *ChemSusChem* 8 (2015) 878–885.
- [10] P. Puthiaraj, S.-S. Kim, W.-S. Ahn, Covalent triazine polymers using a cyanuric chloride precursor via Friedel–Crafts reaction for  $CO_2$  adsorption/separation, *Chem. Eng. J.* 283 (2016) 184–192.
- [11] S. Bhunia, R.A. Molla, V. Kumari, S.M. Islam, A. Bhaumik, Zn(II) assisted synthesis of porous salen as an efficient heterogeneous scaffold for capture and conversion of  $CO_2$ , *Chem. Commun.* 51 (2015) 15732–15735.
- [12] Z. Li, Y. Zhi, P. Shao, H. Xia, G. Li, X. Feng, X. Chen, Z. Shi, X. Liu, Covalent organic framework as an efficient, metal-free, heterogeneous photocatalyst for organic transformations under visible light, *App. Catal. B: Environ.* 245 (2019) 334–342.
- [13] X. Zhu, S.M. Mahurin, S.-H. An, C.-L. Do-Thanh, C. Tian, Y. Li, L.W. Gill, E.W. Hagaman, Z. Bian, J.-H. Zhou, J. Hu, H. Liu, S. Dai, Efficient  $CO_2$  capture by a task-specific porous organic polymer bifunctionalized with carbazole and triazine groups, *Chem. Commun.* 50 (2014) 7933–7936.
- [14] X. Yang, M. Yu, Y. Zhao, C. Zhang, X. Wang, J.-X. Jiang, Remarkable gas adsorption by carbonized nitrogen-rich hypercrosslinked porous organic polymers, *J. Mater. Chem. A* 2 (2014) 15139–15145.
- [15] S. Yao, X. Yang, M. Yu, Y. Zhang, J.-X. Jiang, High surface area hypercrosslinked microporous organic polymer networks based on tetraphenylethylene for  $CO_2$  capture, *J. Mater. Chem. A* 2 (2014) 8054–8059.
- [16] L. Ding, H. Gao, F. Xie, W. Li, H. Bai, L. Li, Porosity-enhanced polymers from hyper-cross-linked polymer precursors, *Macromolecules* 50 (2017) 956–962.
- [17] L. Shao, Y. Sang, J. Huang, Y.-N. Liu, Triazine-based hyper-cross-linked polymers with inorganic–organic hybrid framework derived porous carbons for  $CO_2$  capture, *Chem. Eng. J.* 353 (2018) 1–14.
- [18] Q. Sun, Y. Jin, B. Aguilera, X. Meng, S. Ma, F.-S. Xiao, Porous ionic polymers as a robust and efficient platform for capture and chemical fixation of atmospheric  $CO_2$ , *ChemSusChem* 10 (2017) 1160–1165.
- [19] J. Li, D. Jia, Z. Guo, Y. Liu, Y. Lyu, Y. Zhou, J. Wang, Imidazolium based porous hypercrosslinked ionic polymers for efficient  $CO_2$  capture and fixation with epoxides, *Green Chem.* 19 (2017) 2675–2686.
- [20] A. Samikannu, L.J. Konwar, P. Mäki-Arvela, J.-P. Mikkola, Renewable N-doped active carbons as efficient catalysts for direct synthesis of cyclic carbonates from epoxides and  $CO_2$ , *App. Catal. B: Environ.* 241 (2019) 41–51.
- [21] M. North, R. Pasquale, C. Young, Synthesis of cyclic carbonates from epoxides and  $CO_2$ , *Green Chem.* 12 (2010) 1514–1539.
- [22] N. Wei, Y. Zhang, L. Liu, Z.-B. Han, D.-Q. Yuan, Pentanuclear Yb(III) cluster-based metal–organic frameworks as heterogeneous catalysts for  $CO_2$  conversion, *App. Catal. B: Environ.* 219 (2017) 603–610.
- [23] R.R. Kuruppatharambil, T. Jose, R. Babu, G.-Y. Hwang, A.C. Kathalikkatil, D.-W. Kim, D.-W. Park, A room temperature synthesizable and environmental friendly heterogeneous ZIF-67 catalyst for the solvent less and co-catalyst free synthesis of cyclic carbonates, *App. Catal. B: Environ.* 182 (2016) 562–569.
- [24] W. Ge, X. Wang, L. Zhang, L. Du, Y. Zhou, J. Wang, Fully-occupied Keggin type polyoxometalate as solid base for catalyzing  $CO_2$  cycloaddition and Knoevenagel condensation, *Catal. Sci. Technol.* 6 (2016) 460–467.
- [25] J. Zhu, T. Diao, W. Wang, X. Xu, X. Sun, S.A.C. Carabineiro, Z. Zhao, Boron doped graphitic carbon nitride with acid-base duality for cycloaddition of carbon dioxide to epoxide under solvent-free condition, *App. Catal. B: Environ.* 219 (2017) 92–100.
- [26] L. Liu, S.-M. Wang, Z.-B. Han, M. Ding, D.-Q. Yuan, H.-L. Jiang, Exceptionally robust in-based metal–organic framework for highly efficient carbon dioxide capture and conversion, *Inorg. Chem.* 55 (2016) 3558–3565.
- [27] M. Ding, H.-L. Jiang, One-step assembly of a hierarchically porous phenolic resin-type polymer with high stability for  $CO_2$  capture and conversion, *Chem. Commun.* 52 (2016) 12294–12297.
- [28] S. Ravi, P. Puthiaraj, W.-S. Ahn, Hydroxylamine-anchored covalent aromatic polymer for  $CO_2$  adsorption and fixation into cyclic carbonates, *ACS Sustainable Chem. Eng.* 6 (2018) 9324–9332.
- [29] J. Guipeng, Y. Zhenzhen, Z. Hongye, Z. Yanfei, Y. Bo, M. Zhishuang, L. Zhimin, Hierarchically mesoporous o-hydroxyazobenzene polymers: synthesis and their applications in  $CO_2$  capture and conversion, *Angew. Chem. Int. Ed.* 55 (2016) 9685–9689.
- [30] Z. Dai, Q. Sun, X. Liu, C. Bian, Q. Wu, S. Pan, L. Wang, X. Meng, F. Deng, F.-S. Xiao, Metalated porous porphyrin polymers as efficient heterogeneous catalysts for cycloaddition of epoxides with  $CO_2$  under ambient conditions, *J. Catal.* 338 (2016) 202–209.
- [31] Y. Xie, T.-T. Wang, X.-H. Liu, K. Zou, W.-Q. Deng, Capture and conversion of  $CO_2$  at ambient conditions by a conjugated microporous polymer, *Nat. Commun.* 4 (2013) 1960.
- [32] W. Wang, C. Li, L. Yan, Y. Wang, M. Jiang, Y. Ding, Ionic Liquid/ $Zn$ -PPh<sub>3</sub> integrated porous organic polymers featuring multifunctional sites: highly active heterogeneous catalyst for cooperative conversion of  $CO_2$  to cyclic carbonates, *ACS Catal.* 6 (2016) 6091–6100.
- [33] M.N. Hopkinson, C. Richter, M. Schedler, F. Glorius, An overview of N-heterocyclic carbenes, *Nature* 510 (2014) 485.

[34] R.R. Haikal, A.B. Soliman, M. Amin, S.G. Karakalos, Y.S. Hassan, A.M. Elmansi, I.H. Hafez, M.R. Berber, A. Hassani, M.H. Alkordi, Synergism of carbon nanotubes and porous organic polymers (POPs) in  $\text{CO}_2$  fixation: one-pot approach for bottom-up assembly of tunable heterogeneous catalyst, *App. Catal. B: Environ.* 207 (2017) 347–357.

[35] P. Puthiaraj, W.-S. Ahn,  $\text{CO}_2$ Capture by Porous Hyper-Cross-Linked Aromatic Polymers Synthesized Using Tetrahedral Precursors, *Ind. Eng. Chem. Res.* 55 (2016) 7917–7923.

[36] W.-L. He, C.-D. Wu, Incorporation of Fe-phthalocyanines into a porous organic framework for highly efficient photocatalytic oxidation of arylalkanes, *App. Catal. B: Environ.* 234 (2018) 290–295.

[37] I. Nath, J. Chakraborty, P.M. Heynderickx, F. Verpoort, Engineered synthesis of hierarchical porous organic polymers for visible light and natural sunlight induced rapid degradation of azo, thiazine and fluorescein based dyes in a unique mechanistic pathway, *App. Catal. B: Environ.* 227 (2018) 102–113.

[38] V. Amendola, G. Bergamaschi, M. Boiocchi, L. Fabbrizzi, N. Fusco, The solution stability of copper(I) and silver(I) complexes with N-heterocyclic carbenes, *Dalton Trans.* 40 (2011) 8367–8376.

[39] E. Rangel-Rangel, E. Verde-Sesto, A.M. Rasero-Almansa, M. Iglesias, F. Sánchez, Porous aromatic frameworks (PAFs) as efficient supports for N-heterocyclic carbene catalysts, *Catal. Sci. Technol.* 6 (2016) 6037–6045.

[40] K. Riener, M.J. Bitzer, A. Pöthig, A. Raba, M. Cokoja, W.A. Herrmann, F.E. Kühn, On the Concept of Hemilability: Insights into a Donor-Functionalized Iridium(I) NHC Motif and Its Impact on Reactivity, *Inorg. Chem.* 53 (2014) 12767–12777.

[41] Y. Munaiah, S. Suresh, S. Dheenadayalan, V.K. Pillai, P. Ragupathy, Comparative Electrocatalytic Performance of Single-Walled and Multiwalled Carbon Nanotubes for Zinc Bromine Redox Flow Batteries, *J. Phys. Chem. C* 118 (2014) 14795–14804.

[42] Y.-H. Kim, S. Shin, H.-J. Yoon, J.W. Kim, J.K. Cho, Y.-S. Lee, Polymer-supported N-heterocyclic carbene-iron(III) catalyst and its application to dehydration of fructose into 5-hydroxymethyl-2-furfural, *Catal. Commun.* 40 (2013) 18–22.

[43] Y. Yu, J. Wang, W. Li, W. Zheng, Y. Cao, Doping mechanism of  $\text{Zn}^{2+}$  ions in  $\text{Zn}$ -doped  $\text{TiO}_2$  prepared by a sol-gel method, *CrystEngComm* 17 (2015) 5074–5080.

[44] Q. Chen, M. Luo, T. Wang, J.-X. Wang, D. Zhou, Y. Han, C.-S. Zhang, C.-G. Yan, B.-H. Han, Porous Organic Polymers Based on Propeller-Like Hexaphenylbenzene Building Units, *Macromolecules* 44 (2011) 5573–5577.

[45] K. Song, Z. Zou, D. Wang, B. Tan, J. Wang, J. Chen, T. Li, Microporous Organic Polymers Derived Microporous Carbon Supported Pd Catalysts for Oxygen Reduction Reaction: Impact of Framework and Heteroatom, *J. Phys. Chem. C* 120 (2016) 2187–2197.

[46] M. Errahali, G. Gatti, L. Tei, G. Paul, G.A. Rolla, L. Canti, A. Fraccarollo, M. Cossi, A. Comotti, P. Sozzani, L. Marchese, Microporous hyper-cross-Linked aromatic polymers designed for methane and carbon dioxide adsorption, *J. Phys. Chem. C* 118 (2014) 28699–28710.

[47] X.-M. Hu, Q. Chen, Y.-C. Zhao, B.W. Laursen, B.-H. Han, Straightforward synthesis of a triazine-based porous carbon with high gas-uptake capacities, *J. Mater. Chem. A* 2 (2014) 14201–14208.

[48] X. Gao, M. Liu, J. Lan, L. Liang, X. Zhang, J. Sun, Lewis acid–Base bifunctional crystals with a three-dimensional framework for selective coupling of  $\text{CO}_2$  and epoxides under mild and solvent-free conditions, *Cryst. Growth Des.* 17 (2017) 51–57.

[49] A. Chen, Y. Zhang, J. Chen, L. Chen, Y. Yu, Metalloporphyrin-based organic polymers for carbon dioxide fixation to cyclic carbonate, *J. Mater. Chem. A* 3 (2015) 9807–9816.

[50] K. Pareek, Q. Zhang, R. Rohan, H. Cheng, Highly selective carbon dioxide adsorption on exposed magnesium metals in a cross-linked organo-magnesium complex, *J. Mater. Chem. A* 2 (2014) 13534–13540.

[51] V. Zeleňák, M. Skřínska, A. Zukal, J. Čejka, Carbon dioxide adsorption over amine modified silica: Effect of amine basicity and entropy factor on isosteric heats of adsorption, *Chem. Eng. J.* 348 (2018) 327–337.

[52] A. Demessence, D.M. D'Alessandro, M.L. Foo, J.R. Long, Strong  $\text{CO}_2$ Binding in a Water-Stable, Triazolate-Bridged Metal – Organic Framework Functionalized with Ethylenediamine, *J. Am. Chem. Soc.* 131 (2009) 8784–8786.

[53] J. Wang, W. Sng, G. Yi, Y. Zhang, Imidazolium salt-modified porous hyper-crosslinked polymers for synergistic  $\text{CO}_2$  capture and conversion, *Chem. Commun.* 51 (2015) 12076–12079.

[54] V. Lecocq, A. Graillle, C.C. Santini, A. Baudouin, Y. Chauvin, J.M. Basset, L. Arzel, D. Bouchu, B. Fenet, Synthesis and characterization of ionic liquids based upon 1-butyl-2,3-dimethylimidazolium chloride/ $\text{ZnCl}_2$ , *New J. Chem.* 29 (2005) 700–706.

[55] M. North, R. Pasquale, Mechanism of cyclic carbonate synthesis from epoxides and  $\text{CO}_2$ , *Angew. Chem. Int. Ed.* 48 (2009) 2946–2948.

[56] M.K. Leu, I. Vicente, J.A. Fernandes, I. de Pedro, J. Dupont, V. Sans, P. Licence, A. Gual, I. Cano, On the real catalytically active species for  $\text{CO}_2$ fixation into cyclic carbonates under near ambient conditions: Dissociation equilibrium of  $[\text{BMIm}][\text{Fe}(\text{NO})_2\text{Cl}_2]$  dependant on reaction temperature, *App. Catal. B: Environ.* 245 (2019) 240–250.

[57] J. Chen, H. Li, M. Zhong, Q. Yang, Hierarchical mesoporous organic polymer with an intercalated metal complex for the efficient synthesis of cyclic carbonates from flue gas, *Green Chem.* 18 (2016) 6493–6500.

[58] T. Ema, Y. Miyazaki, J. Shimonishi, C. Maeda, J.-Y. Hasegawa, Bifunctional porphyrin catalysts for the synthesis of cyclic carbonates from epoxides and  $\text{CO}_2$ : structural optimization and mechanistic study, *J. Am. Chem. Soc.* 136 (2014) 15270–15279.